

$^{12}\text{C} + ^{17}\text{O}$ reaction

R. M. Freeman, C. Beck, F. Haas, and A. Morsad

Centre de Recherches Nucléaires and Université Louis Pasteur, 67037 Strasbourg Cedex, France

N. Cindro

*Centre de Recherches Nucléaires and Université Louis Pasteur, 67037 Strasbourg Cedex, France
and Rudjer Bošković Institute, 41001 Zagreb, Croatia, Yugoslavia*

(Received 23 October 1985)

Binary channels of the $^{12}\text{C} + ^{17}\text{O}$ reaction have been studied using a kinematic coincidence technique in the $E_{\text{c.m.}}$ range 16.5 to 29.0 MeV. Angular distributions have been determined for the elastic, the inelastic to the first excited states of ^{17}O and ^{12}C , and the transfer channel to the ground states of ^{16}O and ^{13}C . The angular distributions for the inelastic scattering to the first excited state of ^{17}O , which show strong oscillatory patterns over the whole energy range, could not be reproduced by distorted-wave Born approximation calculations. Structure is observed in the excitation functions of several channels. In particular the structure observed for the inelastic excitation of ^{17}O is similar to that observed in previous γ -ray experiments.

I. INTRODUCTION

The present experiments were stimulated by the discovery of pronounced structure in the yield function of the 0.871 MeV γ transition of ^{17}O excited in the $^{13}\text{C} + ^{17}\text{O}$ collision¹ and by the interpretation of this structure phenomenon as a signature of the Landau-Zener promotion in nuclei.² Subsequent measurements of the $^{12}\text{C} + ^{17}\text{O}$ system again showed structure in the yield of the 0.871 MeV γ ray, with a flat energy dependence for the yield for all other reaction channels. We hence decided to examine more closely the origin of this structure by measuring charged particle data corresponding to these γ transitions. A discussion of the present results in terms of the Landau-Zener promotion of nucleons at avoided crossings in a two-center shell-model (TCSM) diagram is given in the following article. Given the similarity of the TCSM diagrams of $^{13}\text{C} + ^{17}\text{O}$ and $^{12}\text{C} + ^{17}\text{O}$ systems all effort was concentrated on the study of the $^{12}\text{C} + ^{17}\text{O}$ collision which is experimentally the simpler of the two systems.

II. EXPERIMENTAL METHOD

Binary channels of the $^{12}\text{C} + ^{17}\text{O}$ reaction have been studied using a kinematic coincidence technique. The oxygen beam, incident on carbon targets, was furnished by the Strasbourg MP accelerator. The reaction was studied in a first experiment with ^{17}O beam energies ranging from 40 to 51 MeV, mainly in steps of 0.5 MeV; in a second experiment from 44 to 70 MeV in steps of 2 MeV. The carbon targets were approximately $20 \mu\text{g}/\text{cm}^2$ thick.

In the present technique the reaction products were detected in coincidence in two position-sensitive silicon detectors placed on either side of the beam direction. There were modest differences between the detector dimensions and the geometries of the different experiments but, in general, detectors 45 mm long and 15 mm wide

were employed, one placed to cover the angular range 18° to 48° and the other from -68° to -38° (laboratory). For the channels which we have studied this geometry was most suitable where the Q value was close to zero. For each coincidence event the energy and position information from both detectors and the coincidence timing were recorded on magnetic tape. The signals from two small detectors situated at $\pm 7^\circ$ were also recorded on the same tape to serve as monitors.

The position information was calibrated in terms of angle by runs where grids were lowered in front of either detector. The angles corresponding to the grid slits were later measured to a precision of better than 0.2° laboratory, i.e., $\sim 0.5^\circ$ in the center-of-mass frame. Deviations in the beam optics show up sensitively in the ratio of the counting rate between the two monitors and where necessary the angle calibration was corrected. Precise energy calibrations for both detectors followed from the angle calibration and the reaction kinematics.

Once the energy and angle calibrations were determined the data analysis usually proceeded by determining the masses of the detected particles from the following relations which suppose a binary reaction:

$$M_3 = \frac{E_1 M_B}{E_3} \frac{\sin^2 \theta_4}{\sin^2(\theta_3 + \theta_4)}, \quad (1)$$

$$M_4 = \frac{E_1 M_B}{E_4} \frac{\sin^2 \theta_3}{\sin^2(\theta_3 + \theta_4)}, \quad (2)$$

where M_3 , M_4 , E_3 , E_4 , θ_3 , and θ_4 are the masses, energies, and angles of the particles detected in the first and second detector, respectively, E_1 is the incident energy, and M_B the beam mass. Having selected the masses in the outgoing channel an energy spectrum as a function of Q value can be constructed from the conservation of energy relationship:

$$E_3 + E_4 = Q + E_1. \quad (3)$$

There are two ways in which this spectrum can be constructed, either directly from the measured energies E_3 and E_4 , or, alternatively, these energies can be obtained from the position information by fixing the precise values of M_3 and M_4 in formulae (1) and (2). This second method leads to better energy resolutions (of the order of 400 keV FWHM) over most of the angular range. In practice a combination of the two methods was often used. Examples of energy spectra obtained with the second method are shown in Figs. 1 and 2 where the mass M_3 has been selected to be 17 and 16, respectively, corresponding to the inelastic and one-neutron transfer channels. Note that although there is no Z identification involved in this technique other reaction channels like $^{12}\text{B} + ^{17}\text{F}$ and $^{13}\text{N} + ^{16}\text{N}$ are absent from Figs. 1 and 2 because their Q values are too negative.

Angular distributions were obtained with slices corresponding to approximately 0.3° on the position data of the more forward detector. The intensities were transformed to the center-of-mass frame and corrected for the geometry imposed by the coincident condition. This correction was calculated from the dimensions and position of the two detectors and from the kinematics of the reaction under study. The normalization for reactions with the ^{12}C target was first estimated from its nominal thickness and then increased by 25% after comparison of our measurement of the $^{12}\text{C} + ^{16}\text{O}$ reaction at $E_{\text{lab}} = 46$ MeV with the angular distribution of Malmin³ at the same energy. Our absolute cross sections were estimated to be, in general, accurate to 20% though the error may exceed this locally.

III. RESULTS

The relative strength of the mass 17, elastic and inelastic channels can be seen in Fig. 1. The inelastic excitation of the first excited state (0.871 MeV) of ^{17}O is clearly seen but the other two bound states at 3.05 and 3.85 MeV are more weakly excited. The first excited state of ^{12}C (4.44 MeV) is strongly excited. Peaks at more negative Q

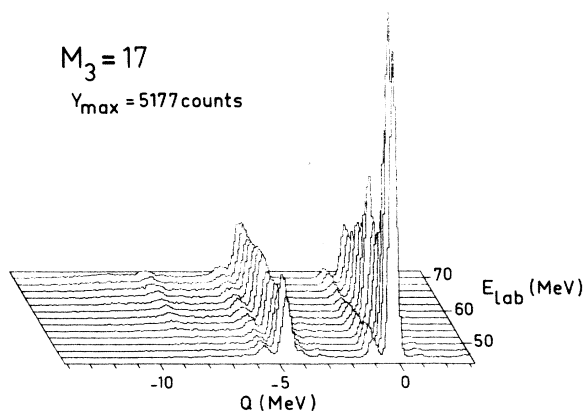


FIG. 1. Evolution of the elastic and inelastic channels of the $^{12}\text{C} + ^{17}\text{O}$ reaction from $E_{17\text{O}} = 46$ to 70 MeV. These spectra, which are approximately normalized, were reconstructed from the coincident events as explained in the text. They correspond to events where particles of mass $M_3 = 17$ are detected in the angular zone $25.2^\circ \leq \theta_3 \leq 28.4^\circ$ of the most forward detector.

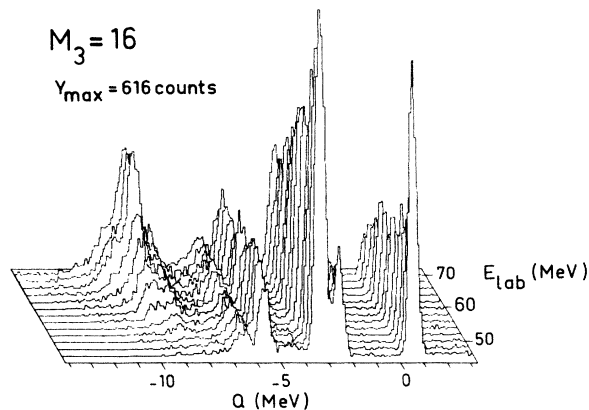


FIG. 2. Evolution with energy of the channels of the $^{12}\text{C} + ^{17}\text{O} \rightarrow ^{13}\text{C} + ^{16}\text{O}$ reaction. The reconstruction of the spectra is identical to that of Fig. 1 except that the mass of the detected particle $M_3 = 16$ in this case.

values arise from the mutual excitation of both nuclei. In our analysis we have determined the angular distributions for the elastic and inelastic ($^{17}\text{O}^*$ 0.871 MeV) channels at all energies and for the inelastic ($^{12}\text{C}^*$ 4.44 MeV) over a wide range of the measurements.

The elastic angular distributions of $^{12}\text{C} + ^{17}\text{O}$ for E_{lab} ranging from 40 to 70 MeV in steps of 2 MeV are shown in Fig. 3. The two regions of the angular distributions arise from the two possible configurations for the coincidence; the forward angles correspond to ^{17}O detected in the first detector and ^{12}C in the second and vice versa for the backward angles. This second angular region was only analyzed for favorable channels, as usually the energy resolutions were poorer and the intensities weak. The forward angle data in Fig. 3 is relatively regular in form and amenable to an optical model analysis. On the other hand the backward angle data shows pronounced irregularities both in cross section and form attesting to the im-

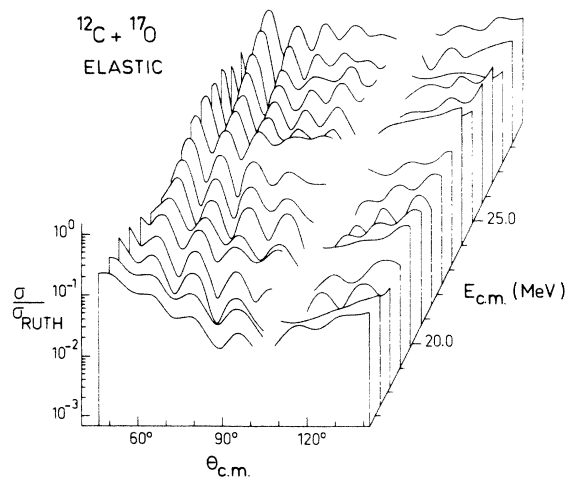


FIG. 3. Elastic angular distributions as a ratio of the Rutherford cross section for $E_{17\text{O}}$ ranging from 40 to 70 MeV in steps of 2 MeV. The two angular regions displayed correspond to the detection of particles of mass $M_3 = 17$ and 12, respectively, in the most forward detector.

portance of processes other than simple potential scattering.

In these experiments we were particularly interested in the angular distributions for the excitation of the 0.871 MeV level of ^{17}O . This transition can be regarded as the promotion of the valence neutron from the $1d_{5/2}$ ground state to the $2s_{1/2}$ excited state. Angular distributions measured over the bombarding energy range are shown in Fig. 4. They present a remarkably strong oscillatory pattern which persists over the whole energy range. Peak-to-valley ratios sometimes exceed an order of magnitude.

The other channel considered in these experiments is the one-neutron transfer channel as shown in Fig. 2. A strong peak is observed at $Q = -3$ MeV corresponding to the feeding of the doublet at 3.85–3.69 MeV of ^{13}C which cannot be resolved with the present resolutions. At more negative Q values the peaks correspond to the excitation of the excited states of ^{16}O and at still more negative values to the mutual excitation of ^{13}C and ^{16}O .

Angular distributions have been extracted at all energies for the $^{12}\text{C} + ^{17}\text{O} \rightarrow ^{13}\text{C}$ g.s. + ^{16}O g.s. reaction. Our measurements overlap with the energy range studied by Debevec *et al.*⁴ for the inverse reaction $^{13}\text{C} + ^{16}\text{O} \rightarrow ^{12}\text{C} + ^{17}\text{O}$. Angular distributions similar to those already published by Debevec were found, and when the factors involved in detailed balance (mainly due to a factor 3 from the spin term) are taken into account, there is also good agreement with the absolute cross sections.

Excitation functions have been determined by integrating the angular distributions over regions sufficiently wide to damp out the angular effects. The energy dependence of the elastic, inelastic, and transfer channels all show some form of structure as seen in Fig. 5. In the large angle elastic scattering [Fig. 5(a)] there are two quite surprisingly sharp structures at 20 and 24 MeV. At 24 MeV it is so narrow that only one point appears in the peak. How-

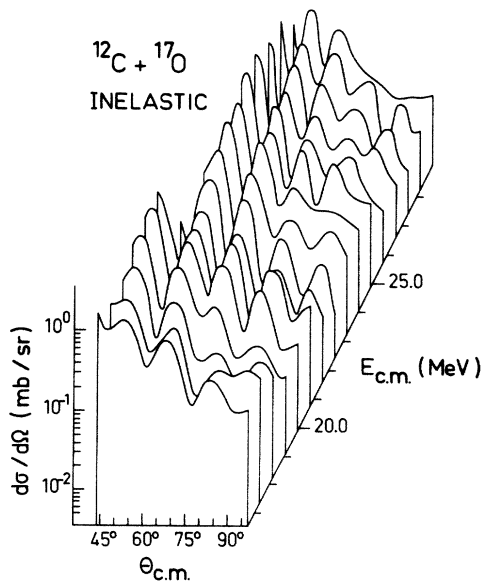


FIG. 4. Angular distributions for inelastic scattering to the 0.871-MeV level of ^{17}O for $E_{17\text{O}}$ ranging from 40 to 70 MeV in steps of 2 MeV.

ever, there are good grounds to believe the anomalous behavior at this energy, as the angular distribution (see Fig. 3) is irregular up to quite forward angles. These two structures occur at energies close to the maxima of the broad structures which are observed for the inelastic scattering to the 0.871-MeV level of ^{17}O [Fig. 5(b)]. This structure in the inelastic channel had already been remarked in earlier γ -ray studies⁵ and in the present results it is observed to continue up to higher energies. The relationship between the γ -ray results and the present observations will be discussed in Sec. V. The partial results for the inelastic scattering to the first excited state of ^{12}C have not been included in Fig. 5 but there is evidence for anomalies in this channel too. The angle-integrated results which we have for this channel resemble the structure which is already apparent in Fig. 1.

IV. DWBA ANALYSIS

We have fitted the angular distributions for the four above-mentioned channels using the DWBA code PTOLEMY. We proceeded first to obtain the optical model parameters for the DWBA calculations by fitting the elastic data starting from the shallow potential used by Malmin^{3,6} for the $^{12}\text{C} + ^{16}\text{O}$ elastic scattering. The radius parameter of the real potential was set fixed at 1.35 fm and all the other parameters allowed to vary to obtain the best fit to the $^{12}\text{C} + ^{17}\text{O}$ scattering. These fits were only made

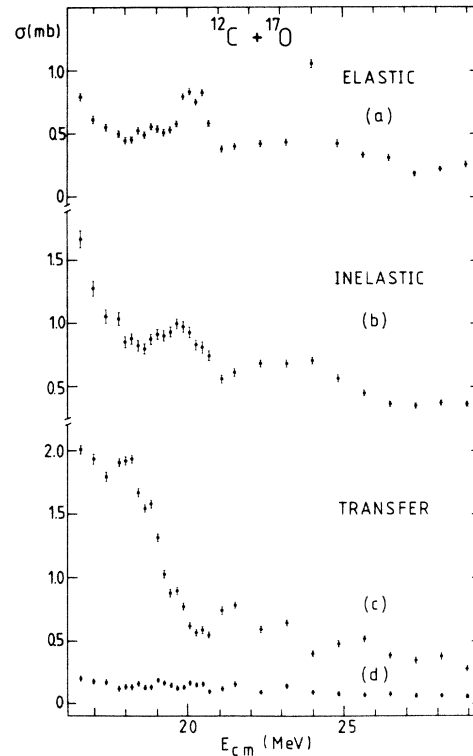


FIG. 5. Excitation function determined by integrating the angular distributions over the indicated center-of-mass angles. (a) elastic scattering $120^\circ \leq \theta \leq 140^\circ$, (b) inelastic scattering to the 0.871 MeV level of ^{17}O $50^\circ \leq \theta \leq 90^\circ$, (c) $^{12}\text{C} + ^{17}\text{O} \rightarrow ^{13}\text{C}_{\text{g.s.}} + ^{16}\text{O}_{\text{g.s.}}$ $50^\circ \leq \theta \leq 90^\circ$, (d) $^{12}\text{C} + ^{17}\text{O} \rightarrow ^{13}\text{C}_{\text{g.s.}} + ^{16}\text{O}_{\text{g.s.}}$ $105^\circ \leq \theta \leq 135^\circ$.

to the forward angle data where the elastic angular distributions vary relatively smoothly with energy. As there are some fluctuations about this smooth behavior the analysis was applied to the data at $E_{\text{lab}} = 50$ and 62 MeV (Fig. 6) where the angular distributions appear to be representative of the whole set. It is notable that a considerably larger diffuseness term in the Woods-Saxon form of the real potential was required for $^{12}\text{C} + ^{17}\text{O}$ than for $^{12}\text{C} + ^{16}\text{O}$ collision, which probably reflect the presence of the loosely bound valence neutron of ^{17}O .

With these new parameters the inelastic and transfer angular distributions were calculated. The deformation parameter for the inelastic scattering were inferred from the lifetimes of the 4.44-MeV state of ^{12}C and the 0.871-MeV state of ^{17}O (Ref. 7). Spectroscopic factors of unity were supposed for the transfer reaction. In all cases the same optical model parameters were used in both the outgoing and incoming channels. Though the calculations tend to predict more pronounced angular distributions, the agreement is otherwise very satisfactory both in form and absolute cross section for the inelastic scattering to the first excited state of ^{12}C and the transfer reaction. On the other hand the calculations fail completely to predict the inelastic scattering to the first excited state of ^{17}O . This is not unexpected as we have used a collective form factor to describe what is essentially a single-particle transition. It is yet to be established how much improvement to the fit could be achieved with coupled-channel calculations. Bohne *et al.*⁸ when confronted with a similar situation for the $^{13}\text{C} + ^{16}\text{O}$ reaction proposed a competing two-step process where the valence neutron is transferred back and forth from the carbon core. Their calculations take specifically into account the single-particle nature of the transition and predict larger cross sections in better agreement with experiment. However there are reasons to doubt whether such a method would reproduce both the

phase and the strong amplitude of the angular distributions for the inelastic scattering to the first excited state of ^{17}O observed in the present experiments.

V. DISCUSSION

The experiments which have been described in this article were directed mainly towards the study of the inelastic excitation of the first excited state of ^{17}O . We have found a strong oscillatory pattern in the angular distributions at all energies and we have not been able to reproduce their phase and cross sections by a DWBA analysis. Moreover, the structure at $E_{\text{c.m.}} \approx 19.5$ MeV which had been observed in previous γ -ray work⁵ for the inelastic channel has been confirmed in the present experiments. These results and their relevance to the Landau-Zener promotion mechanism are discussed in the following article.⁹

At this point it is pertinent to add some remarks about the γ -ray technique which has been used in previous experiments and the particle technique used in the present experiments. Before the results of the two techniques are compared it should be emphasized that there are important differences in so far as what is actually measured. The particle technique which we have used in the present experiments is the more powerful because these are exclusive measurements; however, the data analysis is long and the results limited in angular range. The γ -ray technique is quick and simple to obtain angle integrated intensities but they are also summed over all channels feeding a particular transition. The energy resolutions of the Ge(Li) detectors used in the γ -ray studies are intrinsically much superior to those of the particle experiments but frequently the effective resolution is governed by the Doppler broadening of the γ -ray lines. Using the present particle technique binary channels are selected by the method employed. The transitions from these channels are rarely prominent in the γ -ray spectra which are generally dominated by the more intense transitions from fusion-evaporation processes.

Of the four outgoing channels described in this work only two can be studied by the γ -ray method: those which excite the first excited states of ^{12}C and ^{17}O . In practice only the transitions from the 0.871-MeV level of ^{17}O were studied. Though the 4.44-MeV level of ^{12}C was more strongly excited the detection efficiency for the higher energy transition is smaller and the peak is so Doppler-broadened that it is difficult to extract it from the background. For the reasons given in the preceding paragraph the intensities of the 0.871-MeV γ rays should be considerably greater than the cross sections of Fig. 5(b) and the structure should be to some extent washed out by summation over possible channels. This is what is observed experimentally as the intensities are an order of magnitude larger and the structure less evident in the γ -ray results. Moreover, we are now sure from the particle results that this structure belongs to the simple inelastic scattering channel rather than any other possible process which excites the 0.871-MeV level.

We have attempted to extend the overlap region with the present results by continuing the γ -ray studies up to higher energies. The major difficulty is that the intensity

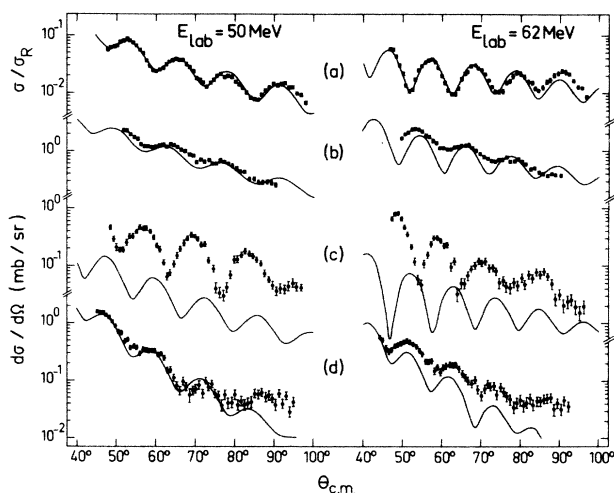


FIG. 6. Comparison between the experimental angular distributions for $E_{^{17}\text{O}} = 50$ and 62 MeV and DWBA predictions for (a) elastic scattering, (b) inelastic scattering to the 2^+ first excited state of ^{12}C , (c) inelastic scattering to the $\frac{1}{2}^+$ first excited state of ^{17}O , (d) $^{12}\text{C} + ^{17}\text{O} \rightarrow ^{13}\text{C}_{\text{g.s.}} + ^{16}\text{O}_{\text{g.s.}}$. Other details concerning these calculations are explained in the text.

of the 0.871 MeV γ rays increases rapidly with energy due to Coulomb excitation of the ^{17}O beam in the target backing, which effectively limits the technique for this particular transition to a relatively low energy region. With unbacked ^{12}C targets the peak would be Doppler-broadened and the intensity difficult or impossible to measure.

The results for the $^{12}\text{C} + ^{17}\text{O} \rightarrow ^{13}\text{C}_{\text{g.s.}} + ^{16}\text{O}_{\text{g.s.}}$ reaction shown in Figs. 5(c) and (d) are of interest because Debevec *et al.*⁴ have suggested that there is a resonance at $E_{\text{c.m.}} = 17.9$ MeV. (In fact Debevec studied the inverse reaction where the corresponding resonant energy is 18.7 MeV.) This resonance was interpreted as the persistence of the well-known 14^+ resonance of $^{12}\text{C} + ^{16}\text{O}$ at 19.7

MeV. There is no serious discrepancy between their experimental results and ours but Debevec *et al.* presented excitation functions at angles close to the maxima of a $[P_{14}(\cos\theta)]^2$ distribution. Their resonantlike results are thus subject to angular dependent effects. In the present angle-integrated results the evidence for a resonance is much less convincing. In the forward angle data [Fig. 5(c)] the structure appears as a step in a region where there is a minimum in the inelastic and elastic excitation functions. In the backward angle data [Fig. 5(d)] it disappears completely. There is evidence for some structure in this channel but no real support for a resonance related to the 19.7 MeV resonance of $^{12}\text{C} + ^{16}\text{O}$.

¹R. M. Freeman *et al.*, Phys. Rev. C **28**, 437 (1983).

²Y. Abe and J. Y. Park, Phys. Rev. C **28**, 2316 (1983).

³R. E. Malmin, Ph.D. thesis, Argonne National Laboratory, 1972; R. E. Malmin, R. H. Siemssen, D. A. Sink, and P. P. Singh, Phys. Rev. Lett. **28**, 1590 (1972).

⁴P. T. Debevec, H. J. Körner, and J. P. Schiffer, Phys. Rev. Lett. **31**, 171 (1973).

⁵C. Beck *et al.*, Nucl. Phys. **A443**, 157 (1985).

⁶S. L. Tabor, Y. Eisen, D. G. Kovar, and Z. Vager, Phys. Rev. C **16**, 673 (1977).

⁷F. Ajzenberg-Selove and C. L. Busch, Nucl. Phys. **A336**, 1 (1980); F. Ajzenberg-Selove, *ibid.* **A281**, 1 (1977).

⁸W. Bohne *et al.*, Nucl. Phys. **A332**, 501 (1979).

⁹N. Cindro, R. M. Freeman, and F. Haas, Phys. Rev. C **33**, 1280 (1986), the following article.